Dissociative X-ray Lasing

Q. Miao,[1,2,*] J.-C. Liu,[3,†] H. Ågren,[1] J.-E. Rubensson,[4] and F. Gel'mukhanov[1]

[1]*Theoretical Chemistry and Biology, School of Biotechnology, Royal Institute of Technology, S-106 91 Stockholm, Sweden*
[2]*College of Physics and Electronics, Shandong Normal University, 250014 Jinan, China*
[3]*Department of Mathematics and Physics, North China Electric Power University, 102206 Beijing, China*
[4]*Department of Physics and Astronomy, Uppsala University, Box 516, S-751 20 Uppsala, Sweden*

(Received 16 April 2012; revised manuscript received 25 June 2012; published 5 December 2012)

X-ray lasing is predicted to ensue when molecules are pumped into dissociative core-excited states by a free-electron-laser pulse. The lasing is due to the population inversion created in the neutral dissociation product, and the process features self-trapping of the x-ray pulse at the gain ridge. Simulations performed for the HCl molecule pumped at the $2p_{1/2} \rightarrow 6\sigma$ resonance demonstrate that the scheme can be used to create ultrashort coherent x-ray pulses.

DOI: 10.1103/PhysRevLett.109.233905 PACS numbers: 42.55.Vc, 41.50.+h, 41.60.Cr, 42.65.Re

In the long history of laser technology, there have been continuous efforts aiming to reach amplification at vacuum ultraviolet and x-ray wavelengths [1,2]. The recent accomplishments of free-electron-laser (FEL) techniques [3–6], and especially the implementation of the principle of self-amplified spontaneous emission, have dramatically changed the experimental prospects for attaining such goals. However, due to the shot-noise start-up in self-amplified spontaneous emission generation of x-ray FEL (XFEL) radiation, the pulses have inherent stochastic character, with rather large variations in wavelength and intensity. This constitutes an obstacle for various applications. One strategy to solve the problem is to use the XFEL pulse to create a population inversion in a medium which then lases in the x-ray region [7–12]. Such an x-ray laser principle based on atomic core level ionization suggested by Rohringer and London [8] was recently demonstrated experimentally [12]. This pioneering result inspires examination of diverse associated mechanisms of x-ray lasing based on XFEL radiation. One alternative is the Raman x-ray laser based on resonant core excitation [9–11]. In this Letter, we investigate x-ray lasing based on resonant core excitation of a molecule to a state which is subject to ultrafast dissociation, i.e., a state in which dissociation precedes the femtosecond core hole decay. Lasing based on photodissociation has earlier been observed in the visible [13,14], UV, and vacuum ultraviolet [15,16] spectral regions.

The lack of feedback mirrors in the x-ray region demands high gain in single-pass pulse propagation. A general obstacle to achieve sufficient gain in this region is that the population inversion propagates slower than the pump pulse. This can be understood as a combination of two effects. First, mainly the front part of the pump pulse creates gain, because field ionization and molecular fragmentation remove molecules from the absorption-emission cycle. Second, this useful part of the pulse is elongated as the pulse is attenuated in the course of propagation. Based on this simple argument, one could think that the different propagation speeds result in a mismatch between the gain and the amplified pulse, and thus the amplification is strongly reduced. Here we predict self-trapping of the amplified pulse in the region of the gain ridge, which is defined by the maximum gain as a function of time and propagation length: We show that the amplified pulse almost follows the same trajectory as the gain ridge. Thereby the energy conversion efficiency of the lasing increases.

Dissociation in core-excited states is a rule rather than an exception [17], and a large number of molecules [18–25] can be used for the dissociative x-ray laser (DXRL). As an example of the proposed lasing mechanism we analyze here the Cl $2p_{1/2} \rightarrow 6\sigma$ excitation of the HCl molecule by an XFEL pulse and the subsequent ultrafast dissociation: $\hbar\omega_p + \mathrm{HCl} \rightarrow \mathrm{HCl}^* \rightarrow \mathrm{H} + \mathrm{Cl}^* \rightarrow \mathrm{Cl} + \hbar\omega + \mathrm{H}$. Because of the ultrafast dissociation, sharp $3s \rightarrow 2p$ atomic lines appear in the inelastic soft x-ray scattering spectra of HCl, excited in the broad $2p^{-1}6\sigma^1$ resonance at $\hbar\omega_p = 201.5$ eV. By tuning the excitation energy $\hbar\omega_p$, the $3s \rightarrow 2p_{1/2}$ or the $3s \rightarrow 2p_{3/2}$ transition can exclusively be selected [26,27]. In the proposed laser scheme, we consider lasing associated with the $3s \rightarrow 2p_{1/2}$ transition at $\hbar\omega = 184.1$ eV. The large width of the 201.5 eV resonance ($\Delta > 2$ eV) and the large spin-orbit splitting (≈ 1.5 eV) relaxes the demands on the energy width of the XFEL pump pulse (around 2 eV is sufficient).

The population dynamics and the lasing are more readily described in the frame ($t = t_\ell - z_\ell/c$, $z = z_\ell$, where c is the speed of light) than in the laboratory frame:

$$\begin{aligned} \left(\gamma(z,t) + \frac{\partial}{\partial t}\right) N_g(z,t) &= -P(z,t), \\ \left(\Gamma(z,t) + \gamma_d + \frac{\partial}{\partial t}\right) N_c(z,t) &= P(z,t), \\ \left(\Gamma(z,t) + \frac{\partial}{\partial t}\right) N_A(z,t) &= \gamma_d N_c(z,t), \end{aligned} \tag{1}$$

These rate equations were solved by using the predictor-corrector method [28]. Here $\Gamma(z,t) = \Gamma + \gamma(z,t)$, $P(z,t) = \gamma_{\rm abs}(z,t)[N_g(z,t) - N_c(z,t)]$, the rate $\gamma(z,t) = \sigma_{NR} I_p(z,t)/\hbar\omega_p$, and the cross section of nonresonant ionization σ_{NR} are assumed to be the same for HCl, HCl*, and Cl*. An energy level diagram of the x-ray dissociative laser is shown in Fig. 1. In the first step of this process, the pump pulse promotes the molecules from the ground state to the core-excited state at a rate $\gamma_{\rm abs}(z,t)$, and the populations of the two states are $N_g(z,t)$ and $N_c(z,t)$, respectively. The core-excited molecular state is depopulated due to radiative and Auger decay at a rate Γ and due to dissociation at a rate γ_d. These processes decrease the concentration of intact molecules $N(z,t) = N_g(z,t) + N_c(z,t)$, while the dissociation increases the population $N_A(z,t)$ of core-excited Cl* atoms. The spontaneous decay of Cl* starts the lasing. The population inversion $N_A(z,t) - N_A^f(z,t)$, where $N_A^f(z,t)$ is the population of the final state of the laser transition, is crucial for the lasing. This is realized by considering the equations for the DXRL intensity $I_L(z,t) \propto \exp[G(z,t)]$ and the gain $g(z,t)$:

$$g = \sigma_A(\omega)[N_A - N_A^f] - \sigma_{NR} N - \sigma_{NR}^{\rm ion} N_{\rm ion}, \qquad (2)$$

where $G(z,t) = \int_0^z g(z',t)dz'$ is the full-trip gain and $\sigma_A(\omega) = \sigma_A \Gamma^2/[(\omega - \omega_{\rm res})^2 + \Gamma^2]$. Here N_0 and $N_{\rm ion}(z,t) = N_0 - N(z,t) - N_A(z,t)$ are the initial concentration of HCl molecules and ions created by the pump pulse, respectively. The cross section for nonresonant absorption by ions is assumed to be the same as for neutral HCl: $\sigma_{NR}^{\rm ion} \approx \sigma_{NR}$. The Doppler broadening neglected here ($k\upsilon \approx 0.0005$ eV $\ll \hbar\Gamma$, $k = \omega/c$) can be significant for higher ω. The main requirement for amplification, $N_A(z,t) - N_A^f(z,t) > 0$, is fulfilled, because the lower lasing level is almost empty ($N_A^f \approx 0$). Until saturation ($I_L \approx 10^{14}$ W/cm^2), the upper state is depopulated mainly due to the Auger decay which produces only ions and no neutral Cl atoms [29,30].

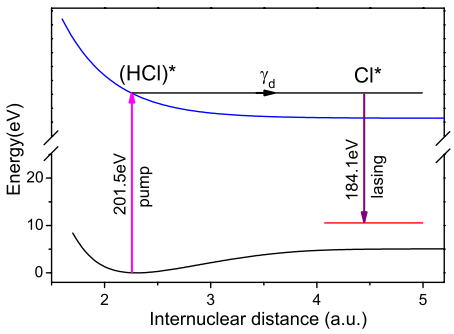

FIG. 1 (color online). An energy level diagram of the X-ray dissociative laser. The XFEL pulse excites the HCl molecule to the $2p^{-1}6\sigma^1$ state in which the molecule dissociates to a hydrogen atom and core-excited Cl atom.

We present simulations for the transition at $\omega = \omega_{\rm res} = 184.1$ eV with $N_0 = 5 \times 10^{19}$ cm^{-3}. We assume that the pump pulse has Gaussian shape $I_p(z,t) = [I_p^0/(1 + z^2/z_R^2)] \exp(-t^2 4\ln 2/\tau_p^2) \exp[-\Lambda(z,t)]$, where I_p^0, τ_p, and $z_R = \pi a^2/\lambda_p$ are the peak intensity, the pulse duration, and the Rayleigh range for the beam radius at the waist a, respectively. The full-trip absorption $\Lambda(z,t) = \sigma_{\rm abs} \int_0^z [N_g(z',t) - N_c(z',t)]dz'$ takes into account the attenuation of the pump intensity in the course of propagation. To make the calculation realistic, we exclusively use parameters extracted from experimental data. The lifetime of the core-excited state is equal to $1/\Gamma = 11$ fs according to experiment [31]. For $\gamma_{\rm abs}(z,t) = \sigma_{\rm abs} I_p(z,t)/\hbar\omega_p$ associated with the $2p \rightarrow 6\sigma$ pump transition, we use $\sigma_{\rm abs} = 1.1$ Mb [32]. The cross section $\sigma_{NR} = 0.38$ Mb was obtained by using the experimental data for HCl [32,33]. Using the Einstein relationship between absorption and spontaneous emission, we estimate the absorption cross section as $\sigma_A = (\lambda^2/4\pi)\Gamma_{\rm sp}/\Gamma \approx 33$ Mb, where $\lambda = 2\pi c/\omega$, $\Gamma_{sp} = w_F \Gamma$ is the rate of the radiative $2p - 3s$ transition, and $w_F = 2.4 \times 10^{-4}$ is the fluorescence yield [34]. The gain for randomly oriented molecules (2) is scaled by the factor 9/5 to take into account the alignment of the core-excited molecules by the pump pulse [17,35]. The rate $\gamma_d \approx \upsilon/\Delta R$ at which the dissociation reaches the region ($\Delta R \approx 1.5$ a. u.) where the potential curve of the core-excited state becomes almost flat is about 0.3 fs^{-1} for $\Delta E \approx 2.5$–5 eV. Here $\upsilon \approx \sqrt{2\Delta E/\mu}$ is the relative velocity of the dissociating atoms. The kinetic energy release during dissociation has been estimated to be $\Delta E \approx 4$ [17] and 2.5 eV [36]. Simulations of g and G for $\Delta E = 2.5$ and 5 eV give similar results within 10%.

Figure 2 shows the population dynamics. The molecules are almost entirely transformed into ions during the pulse. Although the concentration of core-excited atoms N_A is

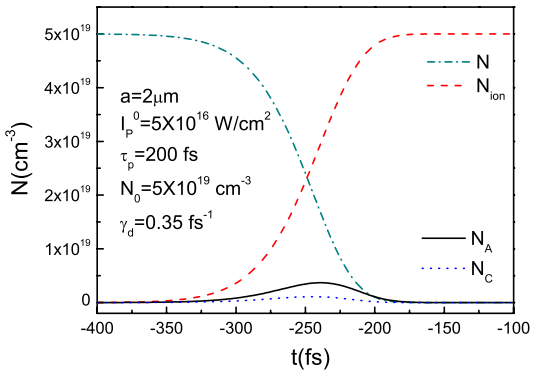

FIG. 2 (color online). Dynamics of the populations at $z = 0$. A significant part of the core-excited molecules "within the pulse" dissociates and forms core-excited Cl atoms creating the inversion of the population. A shift of the maxima of the populations N_c and N_A relative to the top of the pump pulse ($t = 0$) occurs because the intensity of the front of the pump pulse is sufficient to ionize the molecule.

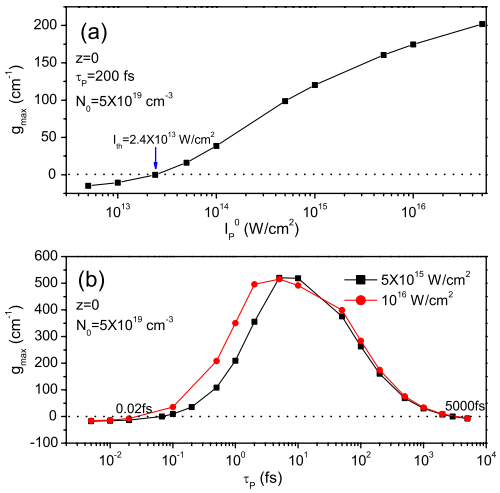

FIG. 3 (color online). (a) Dependence of the gain on the peak intensity of the XFEL pump pulse. The gain is positive when the pump level exceeds the threshold intensity $I_{\rm th}$. (b) Dependence of the gain on the pulse duration.

rather small, it is sufficient to start the lasing if the intensity is higher than the threshold value $I_{\rm th} = 2.4 \times 10^{13}$ W/cm^2 [Fig. 3(a)]. As seen in Fig. 3(b), lasing at $I_p^0 = 10^{16}$ W/cm^2 vanishes when the pulse duration is shorter than 0.02 fs and longer than 5000 fs [this region of the lasing depends on I_p^0 (Fig. 3)]. When the pulse is too short, there are not enough photons to create significant population inversion. When the pulse is too long, the low intensity in the front part of the pulse transforms most of the molecules to ions before the intensity reaches $I_{\rm th}$, and no lasing occurs. The gain creates a coherent, short pulse, due to the exponential dependence of the DXRL intensity on the gain [8–11,37].

We have computed a 2D map [Fig. 4(a)] of the gain $g(z, t)$. Contrary to intuition, the ridge of the gain does not lie on the vertical trajectory $t = t_\ell - z_\ell/c =$ const shown by the white vertical line in Fig. 4. If the DXRL pulse would have propagated with c, this would have created a serious problem, because the overlap of the white line with the gain is small, and, hence, the amplification of the DXRL pulse would have been weak ($G \leq 6.2$; Fig. 5). However, the DXRL pulse propagates with the gain-dependent group velocity [38] $v_g(z, t) = c/[1 + cg(z, t)/\Gamma]$, which affects the intensity [37] according to the equation

$$\left(\frac{\partial}{\partial z} + \frac{1}{u(z,t)}\frac{\partial}{\partial t}\right) I_{\rm L} = g(z,t) I_{\rm L} + J(z,t). \qquad (3)$$

Here $J(z, t) = \Gamma_{\rm sp} N_A(z, t)\hbar\omega\Omega/(4\pi)$, and Ω is the solid angle of the gain region. The "group velocity" of the DXRL pulse $u(z, t)$ in the (z, t) frame is defined by the equation $u^{-1} \equiv dt/dz = dt_\ell/dz - c^{-1} = v_g^{-1} - c^{-1} = g(z, t)/\Gamma$. While v_g is significantly different from c, the group velocity of the pump pulse $v_g^p \approx c$ because $\sigma_{\rm abs} N_g \ll |g|$. According to the simulations, the DXRL pulse tends to

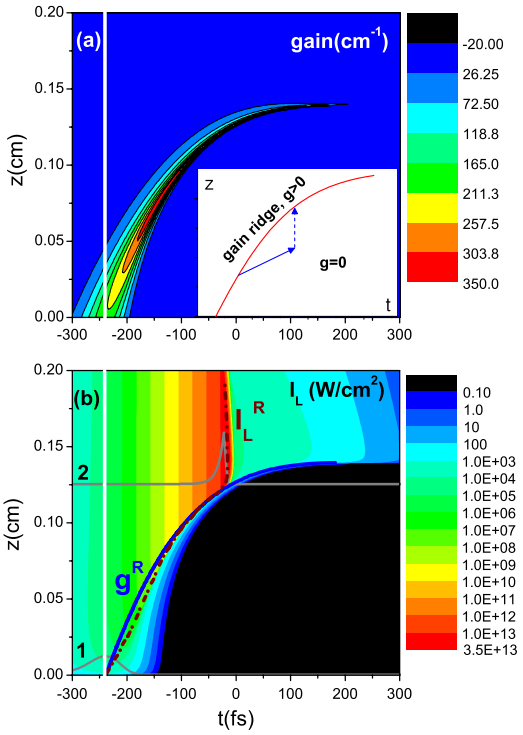

FIG. 4 (color online). Self-trapping of the lasing pulse into the gain ridge. (a) 2D map of the gain distribution $g(z, t)$. The insert explains the self-trapping effect for a simplified situation: $g(z, t) = 0$ everywhere except at the gain ridge. According to simulations $u(z, t)$ is smaller than the slope $dz_{\rm ridge}/dt$, and thus the pulse tends to leave $z_{\rm ridge}(t)$ (solid arrow). However the pulse returns to the gain ridge (dashed arrow)), because $u = \Gamma/g \to \infty$ as soon as it escapes from the ridge. (b) 2D map of the intensity distribution $I_L(z, t)$. The curves 1 and 2 show the DXRL intensity profiles at $z = 0$ ($I_L^{\rm max} = 0.76$ W/cm^2) and at $z = 0.125$ cm ($I_L^{\rm max} = 2 \times 10^{13}$ W/cm^2), respectively. The solid and dashed-dotted curves show the ridges of the gain (g^R) and DXRL pulse (I_L^R), respectively. The vertical white trajectory is going through the maximum of the gain at $z = 0$, $t = -239$ fs. The parameters are the same as in Fig. 2.

escape the gain ridge $z_{\rm ridge}(t)$, because $u(z, t)$ is smaller than the tangent to the gain ridge $dz_{\rm ridge}(t)/dt$ [see the inset in Fig. 4(a)]. However, the increase of $u(z, t) = \Gamma/g(z, t)$ beyond the gain ridge [where $g(z, t)$ is small] forces the pulse to return. The competition between these two opposite trends forces the pulse to follow a trajectory close to the gain ridge. This qualitative picture is in nice agreement with the solution of Eq. (3) shown in Fig. 4(b). This equation with the boundary condition $I_{\rm L}(z = 0, t) = 0$ was solved by using the upwind differencing scheme [28] with the steps of integration $dz = 8.0 \times 10^{-6}$ cm and $dt = 1.467 \times 10^{-2}$ fs. The solid angle of the gain region estimated for a Gaussian beam is $\Omega \approx \lambda_p^2/(\pi a^2) \approx 3.1 \times 10^{-6}$ sr for $a = 2$ μm radius and $\lambda_p = 2\pi c/\omega_p \approx 6.2$ nm. Variation of $\sim$50% of the XFEL profile from the Gaussian beam shape [39] gives the accuracy of our intensity calculation $\delta I_L/I_L = \delta\Omega/\Omega$ of the same order.

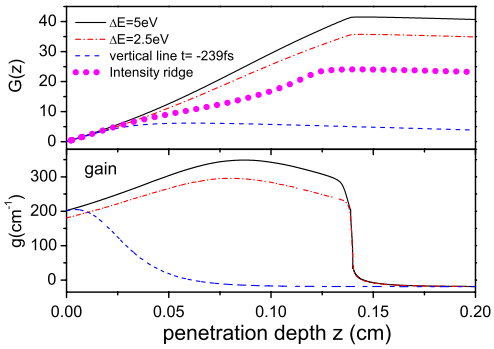

FIG. 5 (color online). Gain, g, and full-trip gain, G, along the gain ridge (solid lines ($\Delta E = 5$ eV), dashed-dotted lines ($\Delta E = 2.5$ eV)). The dotted line displays the full-trip gain along the intensity ridge. The dashed lines show g and G full-trip gain along the vertical white trajectory going through the maximum of the gain at ($z = 0$, $t = -239$ fs, Fig. 4). The parameters are the same as in Fig. 2.

The space- and time-dependent intensity found by solving Eq. (3) is shown by the color field in Fig. 4(b). Time histories at several positions are indicated by the superimposed lines. We find the highest intensity $I_L = 3.5 \times 10^{13}$ W/cm^2 and the energy $E_L \approx 64$ nJ of the DXRL pulse at $z = 0.14$ cm. Figure 4(b) shows that the trajectory of the pulse $z(t)$ almost fully overlaps with the gain ridge $z_{\text{ridge}}(t)$, and the full-trip gain G along the intensity ridge (dotted line in Fig. 5) takes the maximum $G = 24$ which is rather close to the full-trip gain obtained from the solution of Eq. (3) $G = \ln(I_L/I_{\text{seed}}) \approx 20.6$ at $z = 0.14$ cm. The "seed" intensity is estimated by using the solution of Eq. (3) for $g = \text{const}$ [37] (see also Refs. [1,2,40]): $I_{\text{seed}} \approx J/g \approx 3.9 \times 10^4$ W/cm^2. The deviation of the pulse trajectory from the gain ridge is rather small $\Delta t/\tau_p \lesssim 10^{-1}$ [Fig. 4(b)]. This behavior can be described as self-trapping of the lasing pulse at the gain ridge. Apparently, the effect of self-trapping occurs if the following condition is fulfilled: $dz_{\text{ridge}}/dt > u(z, t) = \Gamma/g_{\text{ridge}}$. The pump pulse energy $E_p = 1.3$ mJ ($I_p^0 = 5 \times 10^{16}$ W/cm^2, $\tau_p = 200$ fs, $a = 2$ μm) gives the energy conversion efficiency $E_L/E_p \approx 0.5 \times 10^{-4}$. Figure 5 shows that the gain g and the full-trip gain G along the intensity ridge I_L^R are much stronger than along the trajectory, where $v_g = c$, as shown by the white vertical line in Fig. 4. Thus, the self-trapping effect drastically increases the amplification of the DXRL pulse.

In conclusion, we have proposed a scheme for x-ray lasing in dissociative molecules pumped by an XFEL pulse. It is based on the fact that core excitation of a molecule into a dissociative state can create population inversion in a fragment of the dissociation. The requirements on the duration of the FEL pulse and peak brilliance in the analyzed specific example are fulfilled at FEL in Hamburg (FLASH II) [5] and for other molecules and core excitations realistic conditions are provided by several other existing and planned XFEL facilities. Crucial for the efficiency of the laser scheme is the new predicted effect of self-trapping of the lasing pulse at the gain ridge. The dissociative x-ray laser provides an alternative way to create femtosecond coherent inner-shell x-ray pulses with narrow spectral width, which is vital for numerous applications, for instance, within the field of pump-probe time-resolved spectroscopy.

The research leading to our results has received the support from the Swedish Research Council (VR) and Carl Tryggers Stiftelse (CTS), National Basic Research Program of China (2011CB808100), National Natural Science Foundation of China (Grants No. 10974121 and No. 11204078), and the support by "the Fundamental Research Funds for the Central Universities" (Grant No. 12QN28).

*qmiao@theochem.kth.se
†jicailiu@ncepu.edu.cn

[1] R. C. Elton, *X-Ray Lasers* (Academic, New York, 1990).
[2] P. Jaegle, *Coherent Sources of XUV Radiation: Soft X-Ray Lasers and High-Order Harmonic Generation* (Springer, New York, 2006).
[3] P. Emma *et al.*, Nat. Photonics **4**, 641 (2010).
[4] L. Young *et al.*, Nature (London) **466**, 56 (2010).
[5] K. Tiedke *et al.*, New J. Phys. **11**, 023029 (2009); http://flash2.desy.de/e76656/.
[6] http://www.elettra.trieste.it/FERMI/.
[7] J. Zhao, Q. L. Dong, S. J. Wang, L. Zhang, and J. Zhang, Opt. Express **16**, 3546 (2008).
[8] N. Rohringer and R. London, Phys. Rev. A **80**, 013809 (2009).
[9] Y.-P. Sun, J.-C. Liu, and F. Gel'mukhanov, Europhys. Lett. **87**, 64 002 (2009).
[10] Y.-P. Sun, J.-C. Liu, and F. Gel'mukhanov, J. Phys. B **42**, 201001 (2009).
[11] Y.-P. Sun, J.-C. Liu, C.-K. Wang, and F. Gel'mukhanov, Phys. Rev. A **81**, 013812 (2010).
[12] N. Rohringer *et al.*, Nature (London) **481**, 488 (2012).
[13] J. V. V. Kasper and G. C. Pimentel, Appl. Phys. Lett. **5**, 231 (1964).
[14] E. J. Schimitschek, J. E. Celto, and J. A. Trias, Appl. Phys. Lett. **31**, 608 (1977).
[15] J. C. White and D. Henderson, Phys. Rev. A **25**, 1226 (1982).
[16] K. Ludewigt, H. Schmidt, R. Dierking, and B. Wellegehausen, Opt. Lett. **10**, 606 (1985).
[17] F. Gel'mukhanov and H. Ågren, Phys. Rep. **312**, 87 (1999).
[18] P. Morin and I. Nenner, Phys. Rev. Lett. **56**, 1913 (1986).
[19] O. Björneholm, S. Sundin, S. Svensson, R. Marinho, A. Naves de Brito, F. Gel'mukhanov, and H. Ågren, Phys. Rev. Lett. **79**, 3150 (1997).
[20] M. Magnuson, J. Guo, C. Såthe, J.-E. Rubensson, J. Nordgren, P. Glans, L. Yang, P. Sałek, and H. Ågren, Phys. Rev. A **59**, 4281 (1999).
[21] O. Björneholm *et al.*, Phys. Rev. Lett. **84**, 2826 (2000).

[22] A. Pietzsch *et al.*, Phys. Rev. Lett. **106**, 153004 (2011).
[23] Y.-P. Sun *et al.*, J. Phys. B **44**, 161002 (2011).
[24] K. Ueda *et al.*, Phys. Rev. Lett. **90**, 233006 (2003).
[25] M. Kitajima *et al.*, Phys. Rev. Lett. **91**, 213003 (2003).
[26] J. A. Bearden, Rev. Mod. Phys. **39**, 78 (1967).
[27] C. Såthe, F. Guimarães, J.-E. Rubensson, J. Nordgren, A. Agui, J. Guo, U. Ekström, P. Norman, F. Gel'mukhanov, and H. Ågren, Phys. Rev. A **74**, 062512 (2006).
[28] W. H. Press, S. A. Teukolsky, W. T. Vetterling, and B. P. Flannery, *Numerical Recipes* (Cambridge University Press, Cambridge, England, 2007), 3rd ed.
[29] N. Rohringer and R. Santra, Phys. Rev. A **77**, 053404 (2008).
[30] J.-C. Liu, Y.-P. Sun, C.-K. Wang, H. Ågren, and F. Gel'mukhanov, Phys. Rev. A **81**, 043412 (2010).
[31] R. Feifel *et al.*, Phys. Rev. Lett. **85**, 3133 (2000).
[32] K. Ninomiya, E. Ishiguro, S. Iwata, A. Mikuni, and T. Sasaki, J. Phys. B **14**, 1777 (1981).
[33] W. Hayes and F. C. Brown, Phys. Rev. A **6**, 21 (1972).
[34] M. O. Krause, J. Phys. Chem. Ref. Data **8**, 307 (1979).
[35] L. W. Casperson, W. J. Sandle, A. C. Wilson, D. M. Warrington, and R. J. Ballagh, J. Appl. Phys. **69**, 8005 (1991).
[36] H. Aksela, S. Aksela, M. Ala-Korpela, O-P. Sairanen, M. Hotokka, G. Bancroft, K. Tan, and J. Tulkki, Phys. Rev. A **41**, 6000 (1990).
[37] P. W. Milonni and J. H. Eberly, *Lasers Physics* (Wiley, New York, 2010).
[38] L. Casperson and A. Yariv, Phys. Rev. Lett. **26**, 293 (1971).
[39] A. Barty, R. Soufli, T. McCarville, S. L. Baker, M. J. Pivovaroff, P. Stefan, and R. Bionta, Opt. Express **17**, 15 508 (2009).
[40] A. E. Siegman, *Lasers* (University Science, Mill Valley, 1986).